Supplementary Information

Exploring the potency of currently used drugs against HIV-1 protease of subtype D variant by using multiscale simulations

Md Fulbabu Sk, Rajarshi Roy, Parimal Kar*

Discipline of Biosciences and Biomedical Engineering, Indian Institute of Technology Indore, Simrol Campus, Khandwa Road, Simrol, Indore-453552, Madhya Pradesh, India.

*Corresponding Author: Parimal Kar | Email: parimal@iiti.ac.in | Phone: +91 731 2438700 (Ext. 550)

Table S1: Mean and standard deviation (SD) values for different Cα angles calculated (in the flap tip region of HIV-PR) for all four complexes and apo structures. All values are in degree [°] unit.

	Apo		**ATV/PR**		**DRV/PR**		**LPV/PR**		**TPV/PR**	
Angles	Mean	SD	Mean	SD	Mean	SD	Mean	SD	Mean	SD
49-50-51	109.37	4.44	111.06	4.29	111.27	4.06	110.55	6.11	110.73	3.95
50-51-52	96.15	5.06	96.94	4.55	93.29	3.96	90.41	4.59	93.72	4.05
51-52-53	143.70	8.80	146.06	7.70	141.01	8.77	144.73	6.90	134.58	8.71
49′-50′-51′	92.89	3.82	93.86	5.90	93.72	4.03	95.41	4.30	94.84	3.89
50′-51′-52′	98.10	5.07	107.51	13.30	99.40	5.69	100.06	6.98	99.57	4.43
51′-52′-53′	144.70	6.80	138.54	8.63	143.27	7.00	142.76	7.51	139.15	7.76

(A)

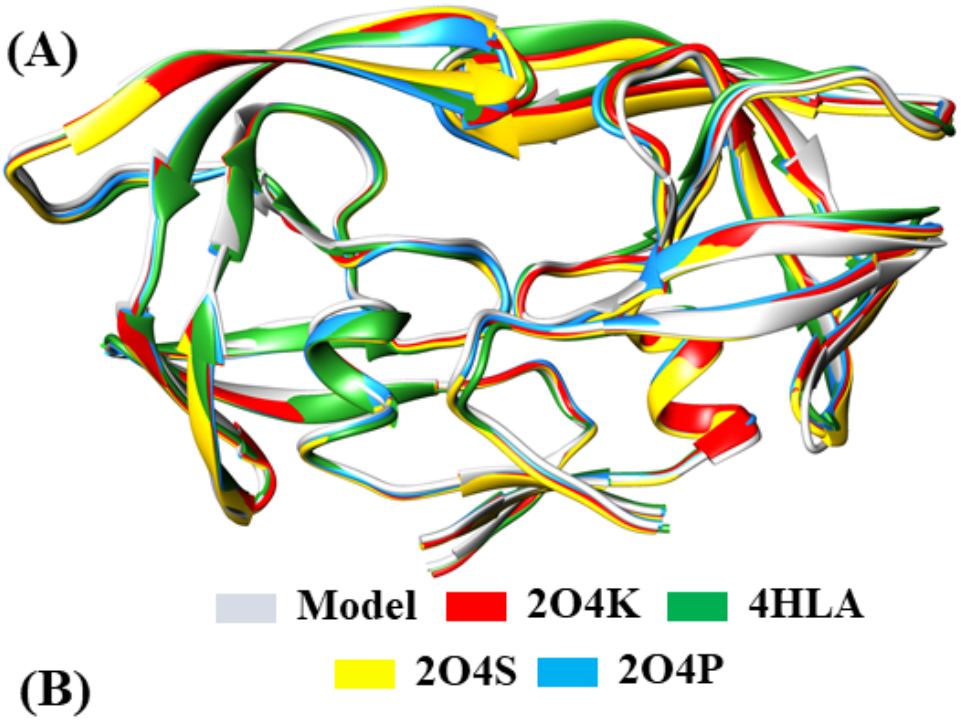

(B)

Templates Structures (Subtype B)	ΔRMSD (Å)
2O4K	0.58
4HLA	0.53
2O4S	0.42
2O4P	0.36

Figure S1: (A) The structural alignment of the model structure (subtype D) along with the respective complexe crystal structure of subtype B. (B) The overall RMSD difference of the model structure and respective complex crystal structures.

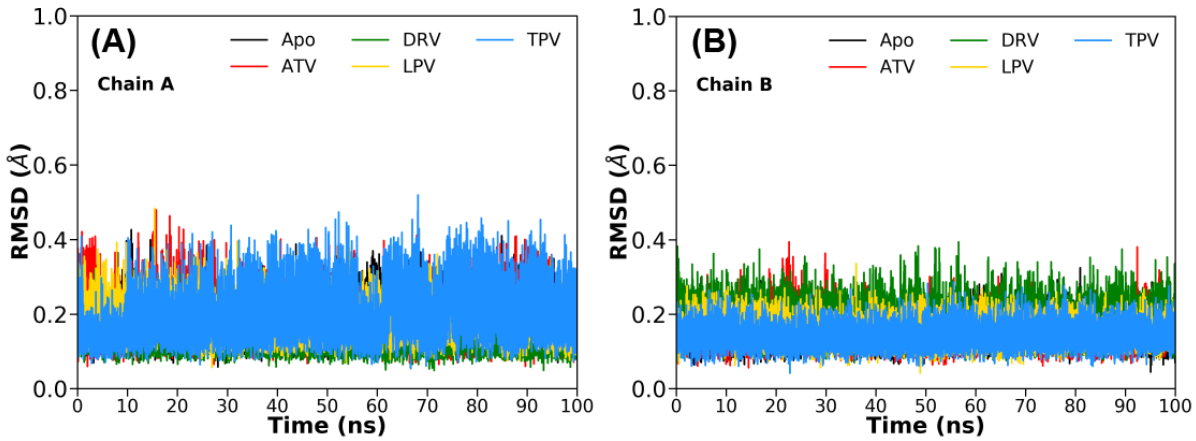

Figure S2: Time evolution of RMSD for active site residues 25-27 (chain A) and residues 25'-27' (chain B) for four inhibitors with HIV-1 subtype D and Apo system.

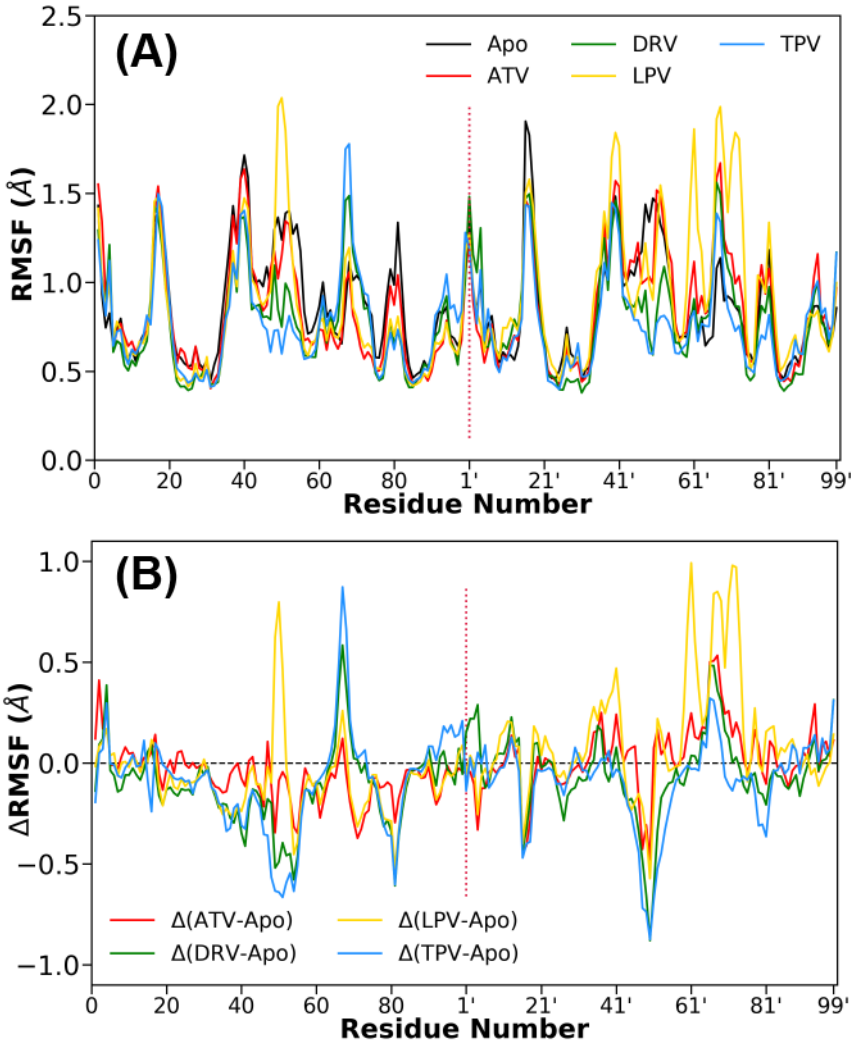

Figure S3: **(A)** Root-mean-square fluctuations (**RMSF**) of PR^D complexed with ATV, DRV, LPV and TPV and Apo systems. Residues 1-99, chain A and 1'-99', chain B. (**B**) The differences of RMSF values of every residue in PR^D of each complexes with respect to Apo system.

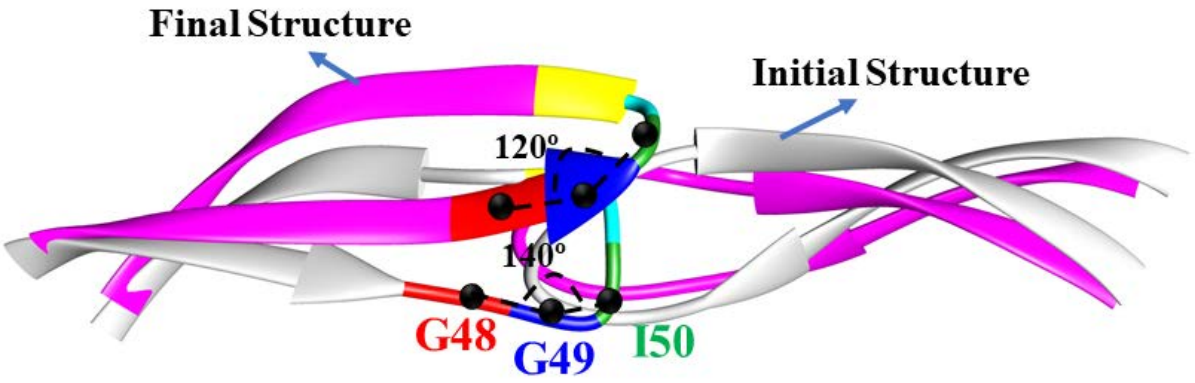

Figure S4: A representative structure of LPV/PR^{D} corresponding to TriCα angle (G48-G49-I50) of 140º deg and 120º.

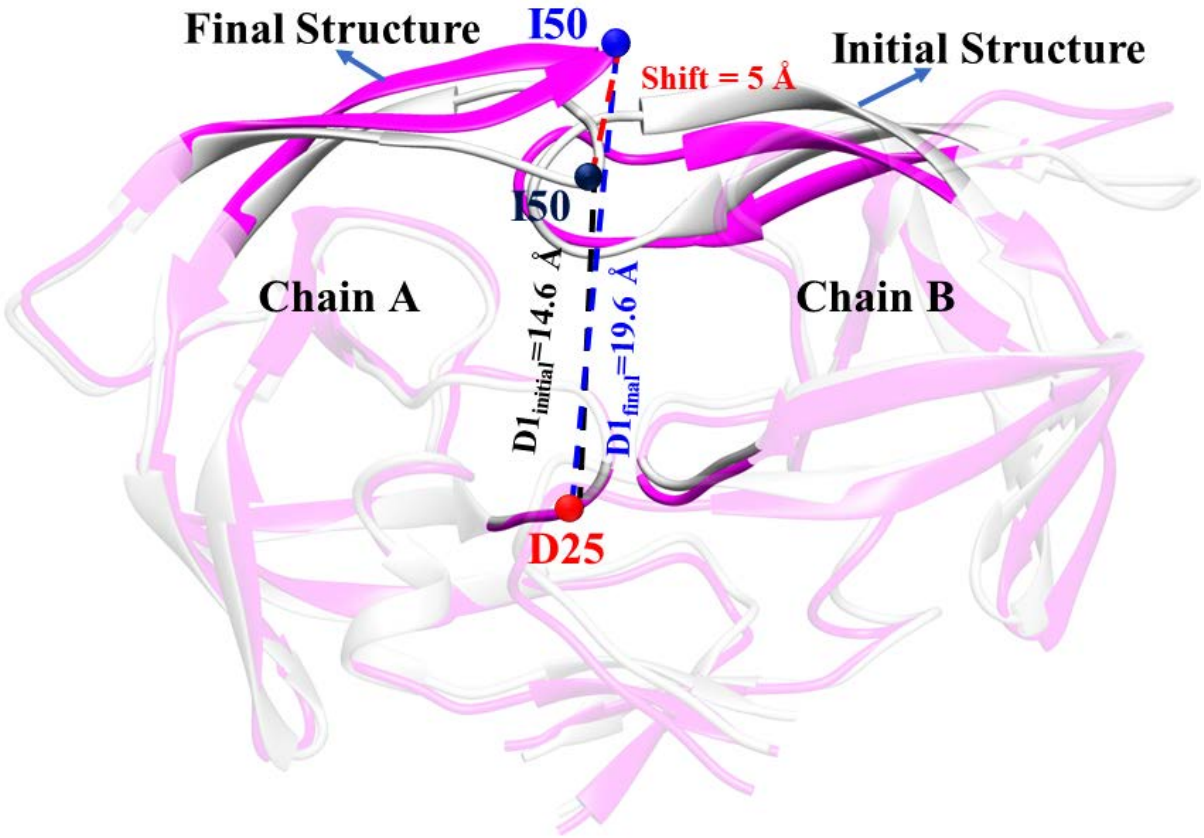

Figure S5: Representative structures of LPV/PR^{D} corresponding to the D25@Cα-I50@Cα distance of 14.6 and 19.6 Å. The magenta and gray colors correspond to the final and inial structure.

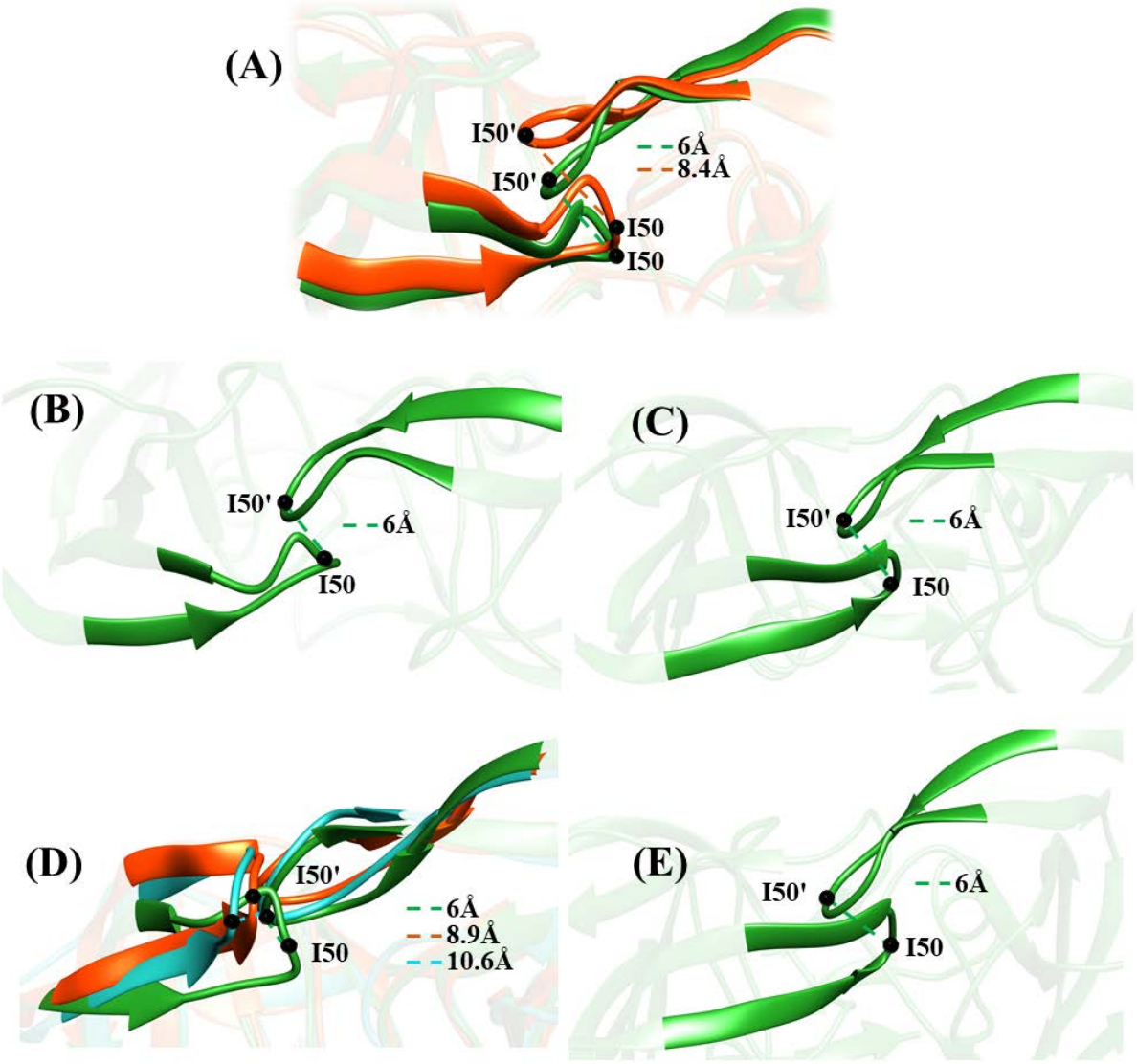

Figure S6: Structures corresponding to the most probable distance between I50@C_α-I50'@C_α. (A) Apo/PR^D, (B) ATV/PR^D, (C)DRV/PR^D, (D)LPV/PR^D, and (E) TPV/PR^D.

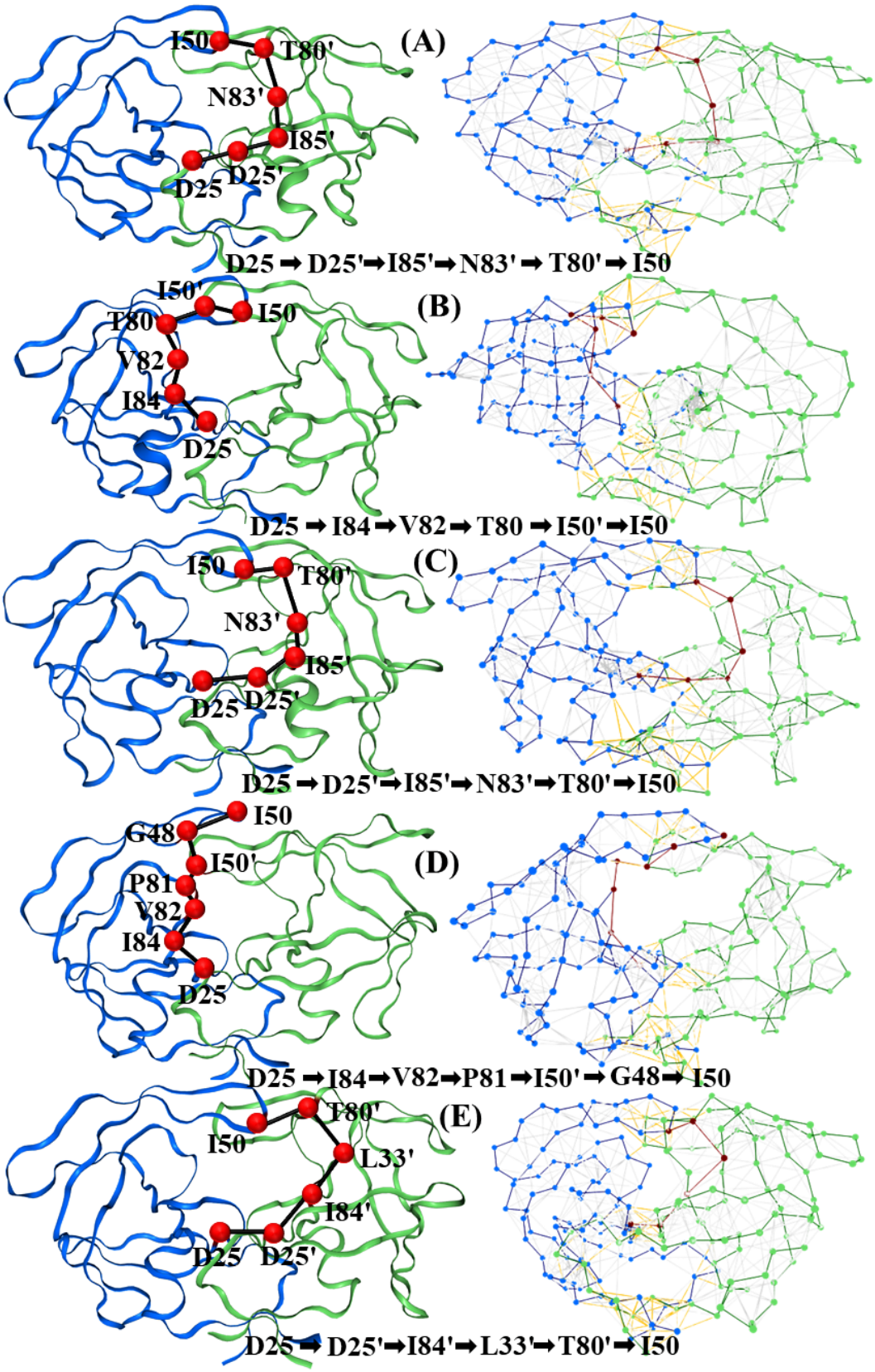

Figure S7: Shortest communication path between the chain A D25 and chain I50 residue or nodes along with network maps investigated via NAPS in (A) Apo, (B) ATV, (C) DRV, (D) LPV and (D) TPV systems.

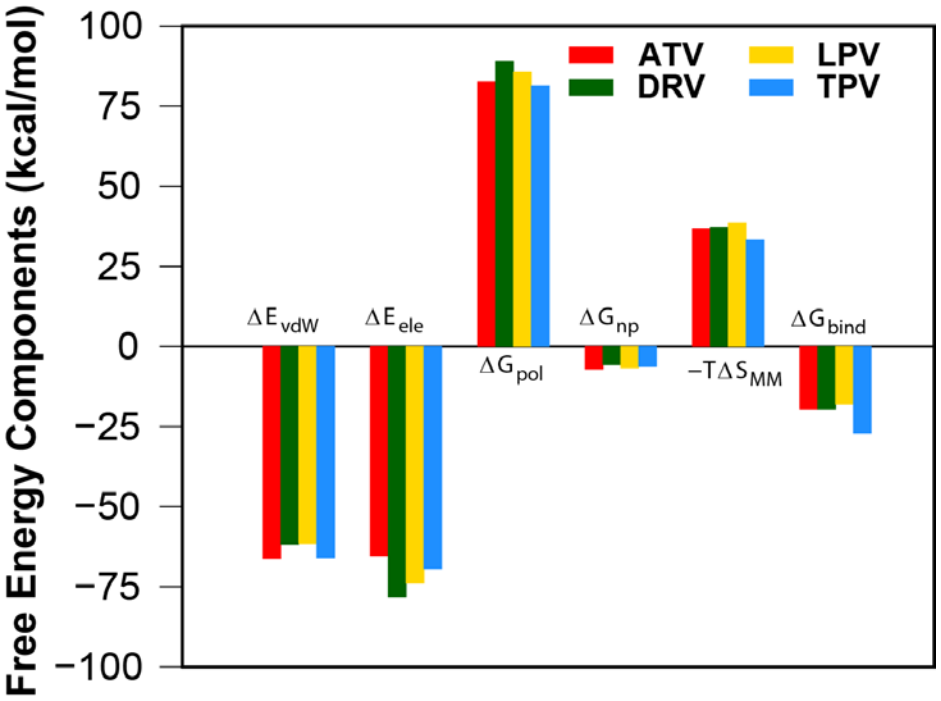

Figure S8: Energy components (kcal/mol) for the binding of drugs to the HIV-1 subtype D. ΔE_{vdW}, van der Waals energy; ΔE_{elect}, electrostatics energy in gas phase; ΔG_{polar}, polar solvation energy; $\Delta G_{nonpolar}$, nonpolar solvation energy; $T\Delta S_{MM}$, configurational entropy contribution and ΔG_{bind}, total binding energy.

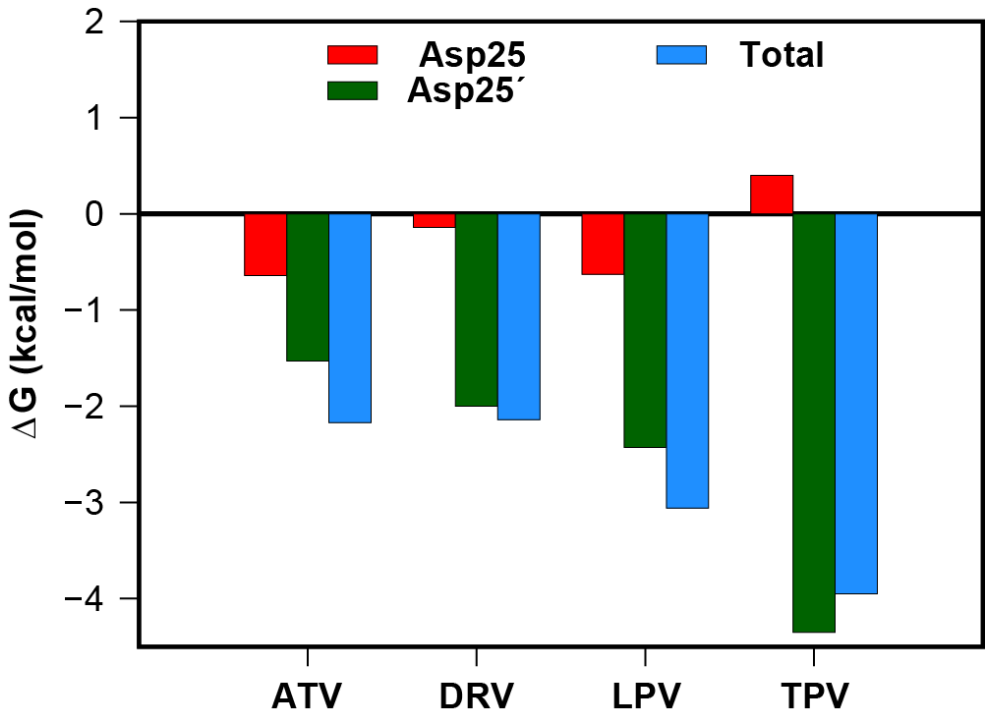

Figure S9: Contribution to the binding free energy from the Asp25/Asp25′ dyad in kcal/mol.

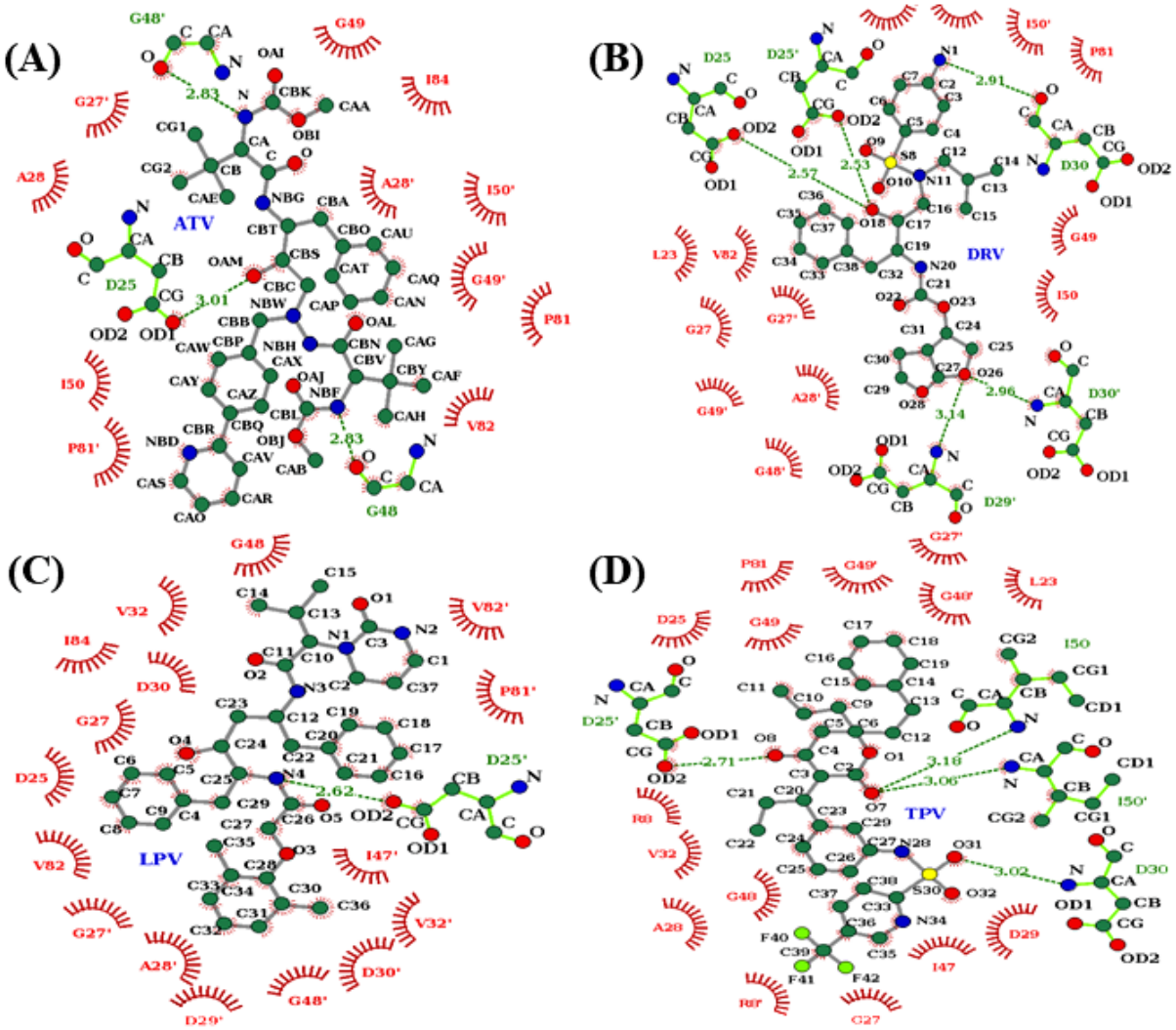

Figure S10: Ligand-protein interaction diagram for the four inhibitors with PRD: (A) ATV, (B) DRV, (C) LPV, and (D) TPV. The plots are generated by using Ligplot+. Hydrogen bonds are shown as green dotted lines. The residues involved in the hydrophobic contacts are represented by red semicircles and residues involved in hydrogen bonds are shown in green. The inhibitors are shown in ball and stick representation.

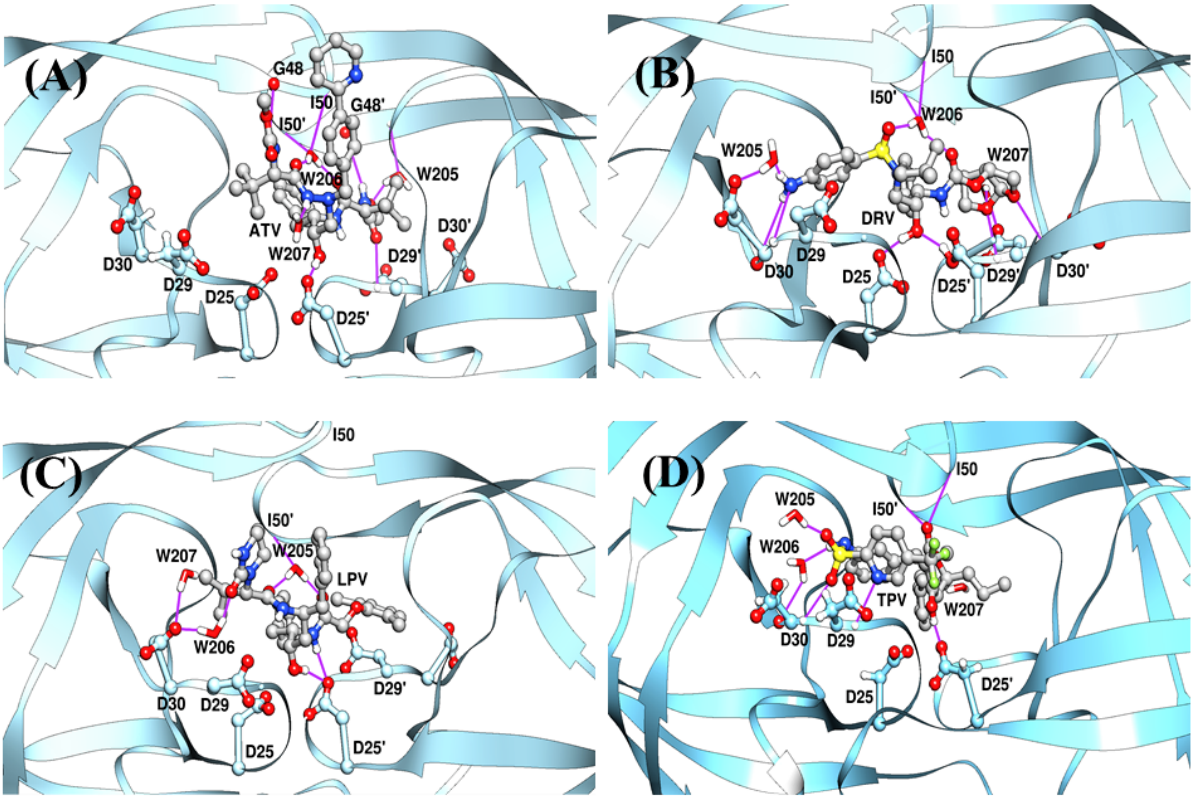

Figure S11: A view of the binding mode of (A) ATV, (B) DRV, (C) LPV and (D) TPV. The dark purple lines represent hydrogen bonds.

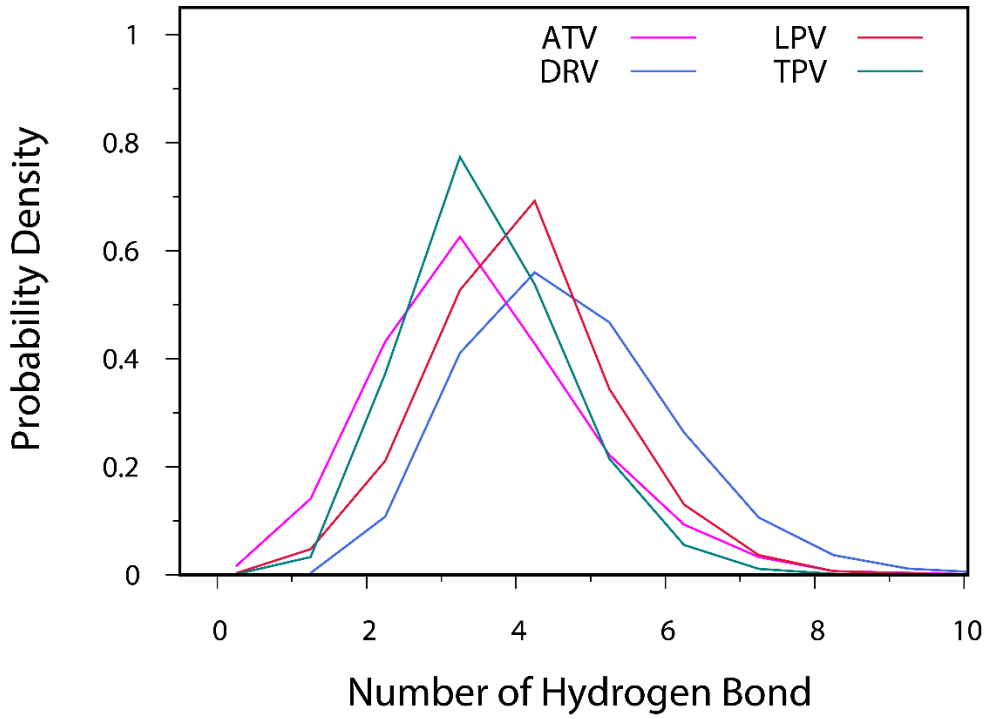

Figure S12: Histogram distribution of the number of hydrogen bond distributions for four inhibitors complexed with PR^D.

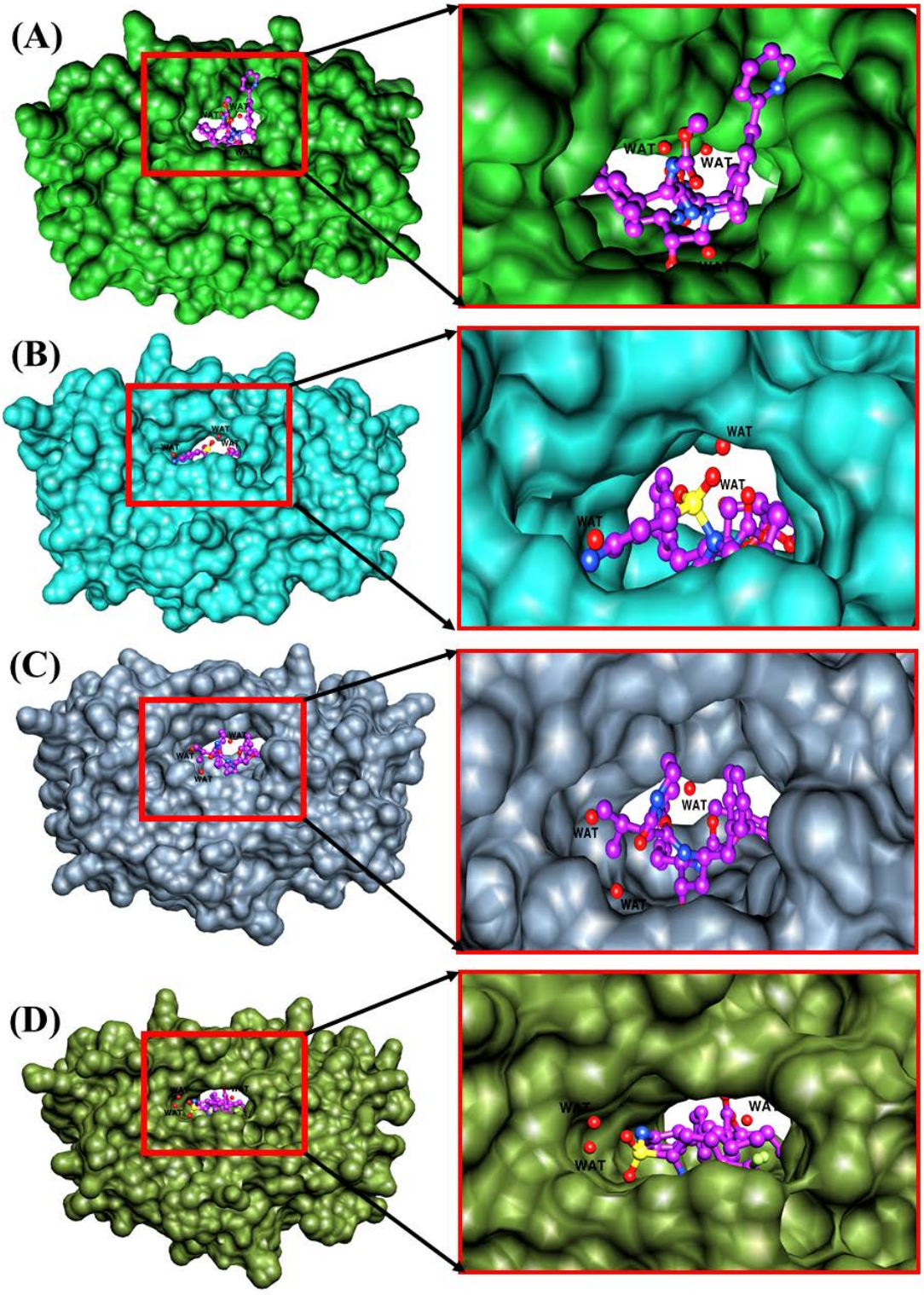

Figure S13: The surface representation of protein and binding pocket of drugs with three water molecules. (A) ATV/PR^{D}, (B) DRV/PR^{D}, (C) LPV/PR^{D}, and (D) TPV/PR^{D}.